PROCEEDINGS, TOUGH Symposium 2006
Lawrence Berkeley National Laboratory, Berkeley, California, May 15–17, 2006

DESIGN AND ANALYSIS OF A GAS THRESHOLD PRESSURE TEST IN A LOW-PERMEABILITY CLAY FORMATION AT ANDRA'S UNDERGROUND RESEARCH LABORATORY, BURE (FRANCE)

Rainer Senger[1], Cristian Enachescu[2], Thomas Doe[3], Marc Distinguin[4], Jacques Delay[4], Bernd Frieg[5]
[1] INTERA Incorporated, 9111A Research Blvd., Austin, Texas, rsenger@intera.com
[2] Golder Associates GmbH, Vorbruch 3, D-29227 Celle, Germany, cenachescu@golder.com
[3] Golder Associates Inc., 18300 Union Hill Rd Suite 200, Redmond WA 98052, tdoe@golder.com
[4] Andra – URL (, RD960 - F-55290, France, Jacques.Delay@andra.fr
[5] NAGRA, Hardstrasse 73, CH-5430 Wettingen, bernd.frieg@nagra.ch

ABSTRACT

A gas threshold pressure test (GTPT) in a deep borehole at Andra's Underground Research Laboratory near Bure, France was conducted to better understand gas transport processes in the low-permeability clay formation under constant rate gas injection conditions. A hydrotest preceding the gas test was performed to estimate the interval transmissivity, static formation pressure, and the flow model in the vicinity of the test section. This information served as the basis for the design and analysis of the gas test to determine the gas threshold pressure of the formation. The gas threshold pressure is typically identified from the pressure buildup curve indicating a deviation from linear increase when the gas starts to migrate into the formation.

The GTPT at Bure showed a sudden pressure decline after continuous gas injection which suggested fracturing of the formation. A second gas injection phase was performed and verified the fracture development and the pressure recoveries following both gas injection phases indicated the same equilibration pressure, which corresponds to the gas threshold pressure of the undisturbed formation.

The GTPT response was analyzed using the two-phase simulator TOUGH2. Even though the standard version of TOUGH2 does not consider coupled mechanical processes associated with the observed fracturing, we used an analytical fracture mechanics analysis to estimate the fracture volume, aperture, and extent. The fracture analysis indicated a horizontal fracture with relatively small lateral extent of a few meters and a maximum aperture of less than 1 mm. The simulation of the initial fracture response used a restart option to incorporate the inferred fracture characteristics in the numerical model. The closure and re-opening of the fracture during the subsequent recovery and second gas injection phase was implemented by calibrating a pressure-dependent permeability relationship for the fracture elements. The analysis further showed that by the end of the first and second recovery phase the fracture did not completely close, characterized by significantly higher permeability (i.e., more than one order of magnitude) than that of the undisturbed rock. The simulations indicated non-linear behavior in terms of fracture closure during the first recovery phase and re-opening during the second gas injection phase. In addition to the fracture behavior that could be quantified, the initial objective of the GTPT was also accomplished. The pressure recoveries following the fracturing could be used in a Horner extrapolation to estimate the gas threshold pressure of the undisturbed formation.

INTRODUCTION

Radioactive wastes and some of the possible canister materials will produce a significant amount of gas due to corrosion (H_2) and degradation processes (CH_4). Gas generation will continue for a long period after repository closure (about 5,000 yrs). Accumulation of the gas leads to a build-up of potentially high gas pressure in the disposal tunnels, if the gas cannot escape through the low permeability host rock. The two-phase flow properties of the host rock are important parameters for the simulation of the gas pressure build-up in the backfilled disposal tunnels and the subsequent release of gas as well as for the assessment of the effects of gas on the long-term performance of the disposal system consisting of engineered and geological barriers.

In 2004 ANDRA (Agence nationale pour la gestion des dechets radioactifs) conducted a GTPT in the borehole EST363 at the Underground Research Laboratory near Bure. The primary objective of the GTPT was to gain understanding of the gas transport processes taking place in the undisturbed Callovian-Oxfordian formation, under constant rate gas injection conditions. In a first step the hydraulic characteristics of the low-permeability clay formation were determined from a hydrotest sequence preceding the gas test, which included (1) the flow model in the vicinity of the test section, (2) the interval transmissivity, and (3) static formation pressure. In a second step, the GTPT was designed to corroborate the hydraulic properties (i.e., transmissivity and formation pressure) obtained from the hydrotest and, more importantly, to determine the gas threshold pressure of the undisturbed formation, and to identify the most appropriate two phase flow parameter model for the formation. This approach is

similar that used by NAGRA during the investigation of the Opalinus clay (NAGRA, 2001), which has similar properties as the Callovian-Oxfordian clay.

The GTPT was designed and subsequently analyzed using the two phase flow code TOUGH2 (Pruess, 1991) and iTOUGH2 (Finsterle, 1999). Modifications were implemented in the TOUGH2 code to account for the effects of borehole closure and fracturing, which were observed during the test and are discussed below.

Background on GTPTs

In a constant-rate gas injection test the deviation of the gas pressure buildup from the wellbore storage period is used to determine the gas threshold pressure (P_{gt}) and the corresponding air-entry pressure (P_e) of the formation, which are defined as:

$$P_{gt} = P_e + P_l$$

where P_l is the liquid or formation pressure. This indicates that the formation pressure has to be known in order to determine P_e from P_{gt}. P_e is a critical parameter for the capillary pressure functions (i.e., van Genuchten, Brooks-Corey). Laboratory data compiled from the literature indicate a linear relationship between air-entry pressure and intrinsic permeability when plotted on a log-log scale, which is described by the following equation (Davies, 1991):

$$P_e = 5.6E\text{-}7 \times k^{-0.346}$$

To apply this relationship, one has to relate the transmissivity estimates from the hydrotest to the intrinsic permeability of the formation. The data for the P_e-k relationship indicates a large uncertainty range and can only provide an initial estimate for the expected P_{gt} for the design of the GTPT in terms of overall pressure buildup and test duration.

For a GTPT in low-permeability rocks the deviation from the linear pressure increase, representing the onset of gas migration into the formation, is difficult to identify and the pressure recovery following shut-in may be very small, requiring an exceedingly long monitoring duration to be able to extrapolate the threshold pressure from the pressure recovery phase.

Deep borehole tests in low-permeability rocks often indicate a composite well-aquifer model characterized by a higher-permeability inner zone due to drilling damage and an outer undisturbed zone of lower permeability and corresponding higher P_e. During gas injection, gas starts to migrate into the inner zone after the gas pressure increase exceeds the P_e of the inner zone (Figure 1). With continued gas injection, pore water is displaced from the inner zone increasing the liquid pressure in the outer zone. The P_{gt} of the outer zone is increased due to the increase in P_l, and could be significantly higher than expected from the P_e-k relationship, assuming constant P_l. In a composite system, only the gas threshold pressure of the inner zone can be identified from the pressure buildup curve. However, the gas threshold pressure of the outer zone, representing the undisturbed formation can be estimated from a Horner extrapolation of the pressure recovery after the gas front extended into the outer zone (Senger et al., 1998).

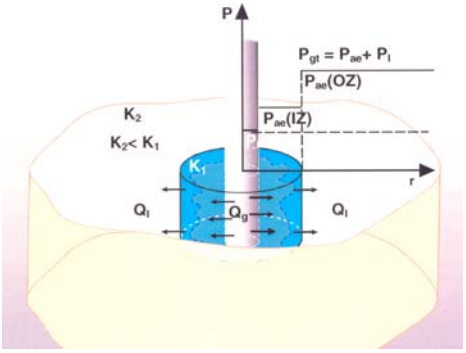

Figure 1. Schematic diagram of gas injection in a composite system.

In addition to the P_e in the capillary pressure function, the relative permeability model can significantly affect the pressure response during a GTPT, particularly in a composite system. Distinguishing gas migration behavior characterized by significant phase interference compared to limited phase interference is important for the safety assessment of gas migration through host rock. The standard Brooks-Corey model (Luckner et al., 1989) shows significant phase interference, whereas in the Grant model having the same liquid relative permeability as the Brooks-Corey model the gas relative permeability, given by:

$$k_{rg} = 1 - k_{rl}$$

indicates no phase interference characteristic of potential preferential gas flow paths in fractured-porous rock.

Finsterle and Pruess (1996), using inverse modeling with iTOUGH2 (Finsterle, 1999), demonstrated that a combination of hydro tests and gas injections improves the identification of two-phase flow parameters by decreasing the uncertainty of the parameter estimates in low permeability, low porosity formation. During the NAGRA (National Cooperative for the Disposal of Radioactive Waste) testing campaign for site characterization of a low and intermediate-level radioactive waste repository in Switzerland, one of the GTPTs in a deep borehole in fractured marl indicated a complex pressure build-up response characterized by a pressure decrease during continuous gas injection. The particular response occurred as the gas started to migrate into the outer zone of a composite system. This response could only

be simulated assuming a Grant relative permeability model (Senger et al., 1998).

TEST DESIGN AND ANALYSIS

The EST363 packer-isolated wellbore interval was at a depth of 490.00 to 495.15 m with a wellbore radius of 0.76 m. The initial design of the GTPT consisted of a constant-rate gas injection phase (GRI1) followed by a recovery (GRIS1). Due to the apparent fracture or flow-path dilation event during GRI1 a second gas injection phase GRI2 was performed followed by a second recovery phase (GRIS2). The entire gas injection sequence was preceded and followed by a pulse withdrawal test (PW1 and PW2), which is shown in Figure 2.

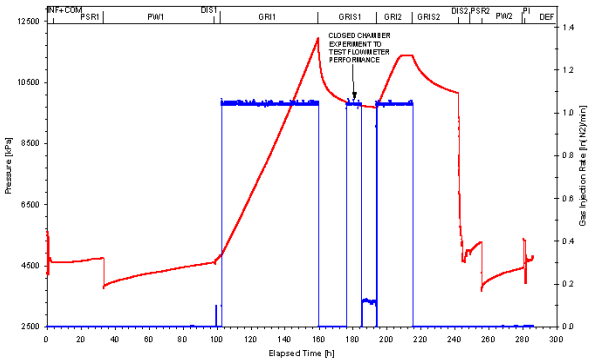

Figure 2. Pressure responses of the entire EST363 test sequence in the test zone and associated gas injection rates.

Hydrotest Analysis

A detailed welltest analysis using a deconvolution approach of the pulse withdrawal test (PW1) data indicated a composite well-aquifer model with a 0.1-m thick higher inner-zone transmissivity and a lower outer zone transmissivity (Fig. 3).

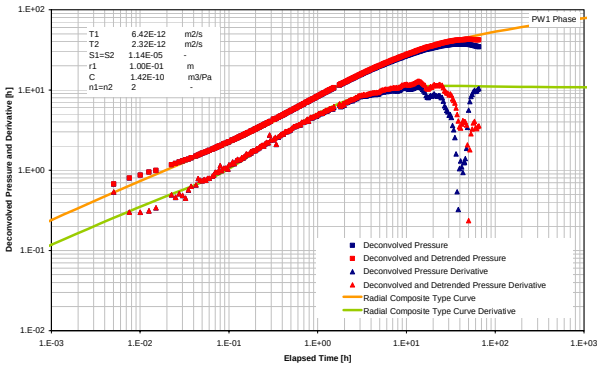

Figure 3. Diagnostic welltest analysis of PW1.

Because of the very low permeability, potential transient effects of the borehole history were taking into account in the analysis of the PW1 sequence, which was done using the nSIGHTs welltest simulator (Intera Engineering Ltd, 2005). The model input with the best-fit hydraulic parameters are summarized in Table 1.

Table 1 Model Input Parameters

Parameter (*with best-fit values*)	**Input**
Test zone compressibility: C_{tz} [Pa^{-1}]	*1.22E-9*
Layer Thickness: b[m]	5.15
Formation pressure: Pi[kPa]	*5060*
Specific storage: Ss_1, Ss_2 [m^{-1}]	1.0E-06
Permeability (inner zone): $k_1[m^2]$	*7.3 E-20*
Permeability (outer zone): $k_2[m^2]$	*3.5 E-20*
Composite discontinuity radius: r_1[m]	*0.1*
Air-entry pressure (inner zone): P_{e1}[kPa]	2,550
Air-entry pressure (outer zone): P_{e2}[kPa]	4,500
Residual gas saturation: S_{gr}	0
Residual water saturation: S_{lr} (fracture el.)	0.85 (0.1)
Brooks-Corey model: shape factor: λ	2
Grant relative permeability:	$k_{rg} = 1-k_{rl}$
Porosity: ϕ (fracture element)	0.1 (0.005)

The composite system was represented by a multi-layer radial mesh that was implemented with TOUGH2, which was used for the simulation of the PW1 response. The variations in the interval pressures during borehole history were represented by discretely prescribed pressures in the test interval, using the restart option in iTOUGH2 (Fig. 4).

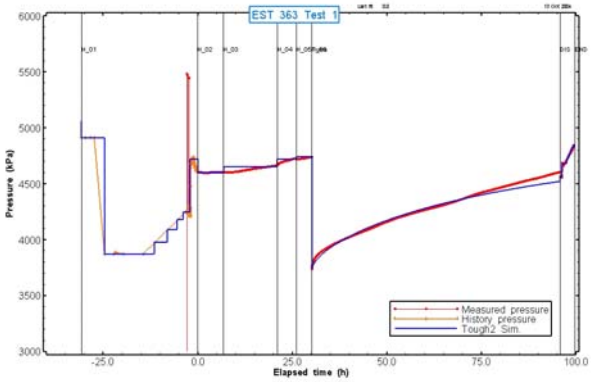

Figure 4. Simulated PW1 response incorporating borehole history.

The simulation of the PW1 sequence compared well with the observed pressures, except at late time, where the measured pressures trend higher than the simulated pressures (Fig. 4). The late-time data were not included in the fitting of the inverse simulation, because the upward trending pressure response at late

time was likely caused by borehole closure, which produced unrealistic high formation pressures (6.5 MPa). Subsequent analyses with nSIGHTs incorporating borehole closure produced similar permeabilities, but lower formation pressures (4.2 – 5.0 MPa) that were consistent with the long-term monitoring pressure data from the electromagnetic pressure gage (EPG) tool in a nearby borehole.

Gas Injection Test

Induced fracturing and borehole closure appear to have influenced the injection phase data. The constant-rate gas injection sequence (GRI1) indicates a near linear pressure increase) to a maximum pressure of 11.9 MPa, followed by a sudden pressure decline (Fig. 2). At close examination, the pressure decline occurred prior to the shut-in, which indicated the induced fracturing of the formation. For the GTPT, a relatively slow pressure buildup is required to better identify the onset of gas migration into the formation, based on a deviation from linear pressure increase representing wellbore storage of the gas filled test interval.

As to borehole closure, the diagnostic plot of the GRI1 response indicates a gradual increase in slope of the *dP* curve (Fig. 5). This trend could be caused by either borehole closure or by a drift in the gas flow meter for flow rate measurements at higher pressure. The calibration of the gas flow meter was tested during a gas injection experiment in a closed tubing (outside of the borehole) as indicated by the monitored gas injection rate during the GRIS1 shut-in period (Fig. 2). The verification of the measured gas flow rates suggested that borehole closure was the most likely mechanism of the observed upward trend in the *dP* curve. The diagnostic plot of the GRI1 sequence (Fig. 5) in terms of the derivative of the pressure buildup (*dP'*) indicates a noticeable deflection after about 23 hours at a *dP* of about 2.6 MPa. This pressure corresponds approximately to the air-entry pressure of the inner zone based on the P_e-k relationship above, indicating the onset of gas flow into the inner zone.

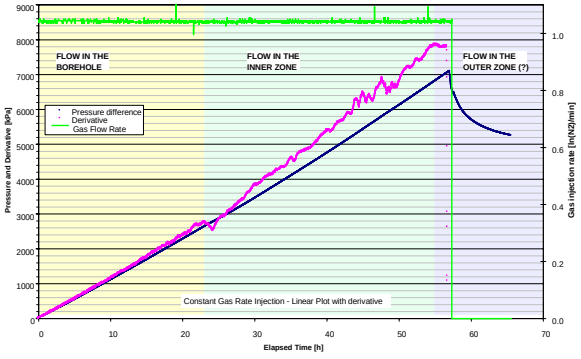

Figure 5. Diagnostic plot of GRI1 pressure response.

The estimated permeability of the outer zone is lower than that of the inner zone by a factor of about two (Tab. 1), which corresponds to a value of P_{e2} = 3.28 MPa, compared to P_{e1} = 2.55 MPa (Tab. 1). However, the pressure buildup did not indicate any distinct deviation between 3.0 and 9.0 MPa (Fig. 5). There are some fluctuations in the derivative between 6.0 and 7.0 MPa, but only prior to the fracture event was there a noticeable deviation in the derivative curve at about 8.0 MPa, suggesting the onset of gas migration into the outer zone. However, this "apparent" gas threshold pressure is increased due to the increase in liquid pressure associated with the pore-water displacement from the inner zone. The increase in the liquid pressure in the outer zone causes a reduction in effective stress which probably helped induce fracturing at a much lower frac pressure than those observed from standard hydrofract experiments in nearby boreholes.

The gas threshold pressure of the outer zone can be obtained from the recovery periods following the GRI1 and GRI2 injection sequences (Fig. 2). The Horner extrapolation of the recovery phases indicated a P_{gt} of about 9.5 MPa (Fig. 6), which corresponds to a P_{e2} of 4.5 MPa for the outer zone, based on a static formation pressure of about 5.0 MPa. The estimated P_{e2} of 4.5 MPa is representative of the undisturbed formation, despite the fracture event that occurred at the end of GRI1 and fracture reopening during GRI2.

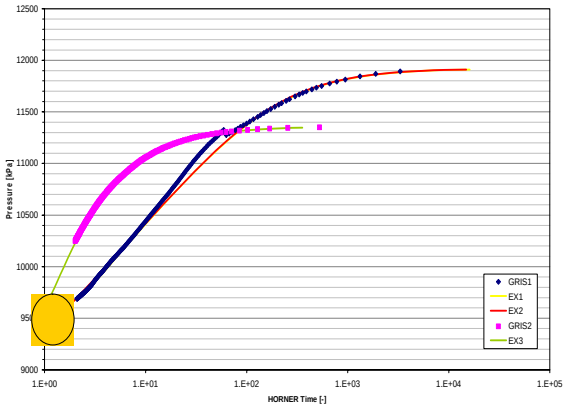

Figure 6. Horner extrapolation of GRIS1and GRIS2 pressure recoveries.

Hydraulic Fracture and Volumetric Analysis

The approach of the fracture analysis is based on rock mechanics and linear elastic fracture mechanics (Davis, 1989) and is described in detail in Senger et al. (2005). The conceptual model for the fracturing event involved the creation of a fracture toward the end of the first injection cycle at the peak pressure (P_{f1}) of 11.9 MPa. The pressure in the zone rapidly fell as the fracture propagated and gas started to flow into the rock over the newly created fracture face.

The peak pressure during GRI2 (P_{f2}) of about 11.38 MPa and associated steady gas flow indicates fracture opening. This pressure is less than the interpreted minimum stress at this depth, suggesting no further propagation of the fracture. That is, the produced fracture adds a gas filled volume in direct contact with the gas filled wellbore volume. The volume change, representing the gas-filled fracture volume, can be estimated from P_{f1}, P_{f2} and the wellbore volume at the time of fracture initiation.(V_1 = 42 liters) according to Boyle's law as 2.02 liters.

The fracture aperture was estimated based the mechanical properties of the rock (shear modulus, Poisson ratio, fracture toughness), and the effective stress in the fracture, as described in greater detail in Senger et al. (2005). Given the uncertainty in mechanical properties, we established a range in maximum fracture aperture of between 0.5 and 0.7 mm at the borehole wall and fracture radius range of 1.0 and 2.4 m. The aperture decreases as a function of distance from the borehole to zero at the fracture tip based on the mechanics of a pressurized crack (Davis, 1989).

TOUGH2 MODELING OF THE GTPT

The numerical model for the simulation of the GTPT is represented by a five-layered radially-symmetric mesh. The thickness of the model represents the total interval thickness of 5.15 m. The potential fracture was represented by a 0.15-m thick layer in the center of the interval, with adjacent layers of 0.75 m and 1.75 m thickness. Horizontal grid spacing increased logarithmically with a minimum of 0.001 m at the wellbore., the radial mesh represents a composite well-aquifer model prior to the fracture event at the end of GRI1with input parameters summarized in Table 1.

Constant Rate Gas Injection Sequence 1 (GRI1)

The effect of apparent borehole closure during GRI1 was incorporated by implementing a linear decrease in the test-interval volume from 59 liters to 42 liters, which produced a very good fit of the observed pressure increase during GRI1 (Fig. 7). The observed onset of gas flow into the inner zone was defined by the Brooks-Corey model with the inferred air entry pressure of P_{e1} = 2.55 MPa. The diagnostic plot shows the deviation in the derivative (Fig. 7), indicating the onset of gas flow into the inner zone. The onset of gas flow into the outer zone was assumed to occur just before the fracture event (Fig. 5). For the outer zone, the P_{e2} value of 4.5 MPa extrapolated from the gas threshold pressure for the outer zone (Fig. 6) was used in the model. The required increase in liquid pressure (i.e., formation pressure) was simulated by calibrating the residual water saturation in the two-phase flow model which largely controls the amount of water that is displaced by the injected gas from the inner zone into the outer zone. In order for the simulation to show gas migration into the outer zone before the fracture event, the residual water saturation had to be increased to 0.85.

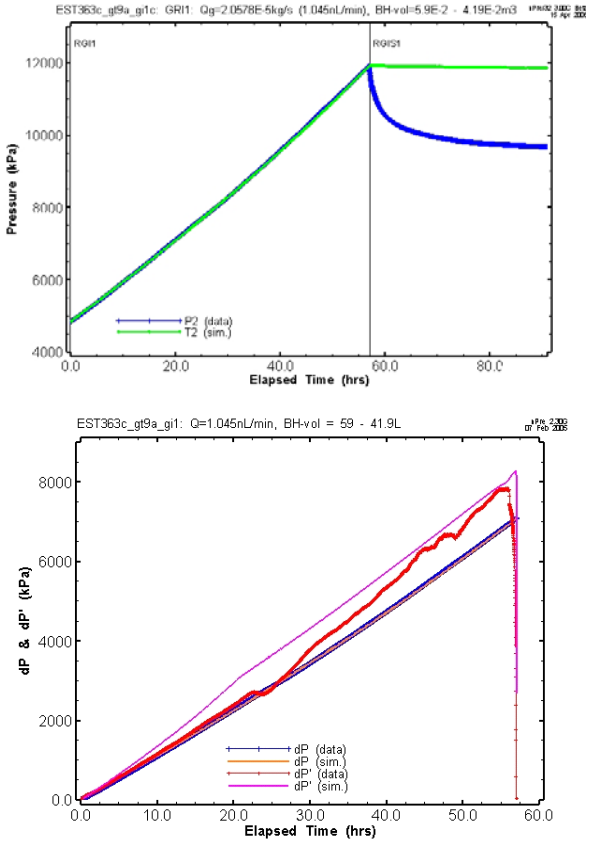

Figure 7. Cartesian plot of GRI1 and GRIS1 (top) and diagnostic plot (bottom) of the simulated and observed GRI1repsonse.

Recovery Sequence 1 (GRIS1)

Without fracture development, the simulated pressure recovery would show only a very small pressure recovery as indicated in the Cartesian plot in Figure 7. As discussed above, the pressure recovery can be used to extrapolate the gas threshold pressure of the outer zone. However, such low permeabilities, require a very long recovery. The comparison with the measured response indicates that a fracture event occurred resulting in a significant pressure recovery during GRIS1 (Fig. 7).

The fracture event was simulated by a restart using the conditions at the end of GRI1 as initial conditions. The estimated fracture aperture (b) was implemented as equivalent porosities (ϕ_e) over the estimated fracture length for the 0.15-m thick elements (b_e) in the center of the test interval, defined

as $\phi_e = b/b_e$ (Fig. 8). Furthermore, a capillary pressure corresponding to the largest fracture aperture (0.7 mm) was used as air-entry pressure (P_{ef} = 200 Pa) for the fracture elements.

The model did not explicitly simulate the mechanical processes associated with fracture opening and potential fracture propagation. Instead, the model represented the fracture opening and propagation by advective-diffusive displacement of the pore water from the fracture element into the adjacent undisturbed formation. For this, the relative permeabilities of the elements representing the extent of the fracture are represented by a Grant model, indicating high gas mobility.

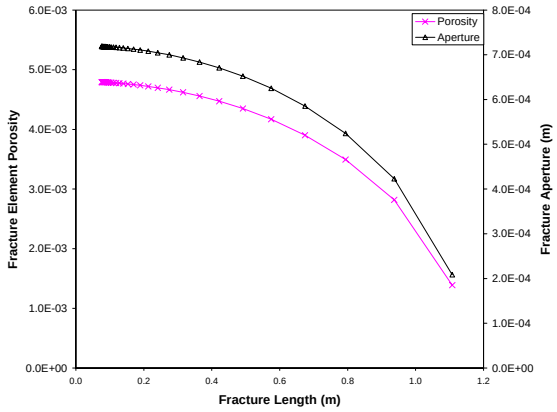

Figure 8: Estimated fracture aperture and corresponding fracture porosity using in the model.

Furthermore, by setting the air-entry pressure of the fracture elements at a very low value, a significant suction gradient is created for the pore water from the fracture into the adjacent formation. One rationale for this approach is the compensation of TOUGH's need for initial water saturation in the fracture with the mechanical reality that the fracture is gas-saturated from its creation. Hence, the two-phase flow properties of the fracture are set to make negligible the effects of the model's initial fracture-water content.

The changes in fracture properties during the different test sequences following the initial fracture event were represented by pressure-dependent permeability functions which were calibrated for the different test sequences. These changes were considered representative of fracture closure and other restrictions in the gas flow during GRIS1 and GRIS2 and reopening of the fracture during GRI2.

A pressure-dependent permeability relationship was implemented for the fracture element, defined by an initial pressure (P_1) representing the onset of fracture opening and corresponding permeability increase, and an upper pressure (P_2) corresponding to a maximum fracture permeability:

$$k_f = k_0 \qquad P < P_1$$
$$k_f = k_0(1+(kfact-1)(P-P_1)/(P-P_2)) \qquad P_1<P<P_2$$
$$k_f = k_0 \times k\,fact \qquad P > P_1$$

The start of the GRIS1 sequence corresponds to the sudden pressure drop indicating the fracturing or pathway dilation of the formation. However, gas injection continued for about 15 minutes, before it was stopped, which was accounted for in the simulation.

A series of simulation was performed to evaluate different parameters, such as the permeability factor and the pressure range over which the fracture permeability decreased during GRIS1. More importantly, to reproduce the shape of the pressure response, the fracture volume had to be increased, by increasing the fracture length from 2.4 m that was based on the hydraulic fracture analysis to 3.4 m. Increasing the fracture length was considered appropriate, considering the potential uncertainties in the parameters for the analytical fracture mechanics model. Note that the simulation of the sequences following the fracture event did not consider borehole closure, since the volumetric calculations did not indicate a further decrease in borehole volumes.

The simulation with a 3.4-m long fracture produced a very good fit of the GRIS1 response (Fig. 9), using a pressure-dependent permeability function with a permeability factor of *kfact* = 2,500 indicating a pressure increase by more than three orders of magnitude over a pressure range between P_1 = 9.6 MPa and P_2 = 12MPa.

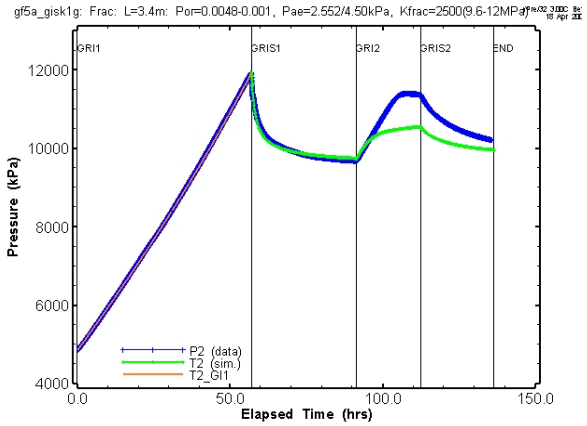

Figure 9: Simulated injection pressures for GRIS1, GRI2, and GRIS2 (calibration of GRIS1response).

The lower pressure range (P_1= 9.6 MPa) indicates that at the end of GRIS1 (P = 9.67 MPa), the fracture is not completely closed and has significant permeability (k_f = 2.6E-18 m^2), which is nearly two orders of magnitude greater than that of the

undisturbed outer zone permeability (k = 3.5E-20 m^2). That is, given the linear relationship of the pressure-dependent permeability, the permeability rapidly increases over small pressure increments above the 'opening pressure' of 9.6 MPa. resulting in a simulated pressure buildup during GRI2 noticeably lower than the observed response (Fig. 9). The fracture permeability is apparently too high at the beginning of GRI2, but not high enough toward the end of GRI2 to reproduce the flattening of the pressure response.

Constant Rate Gas Injection Sequence 2 (GRI2)

In a first simulation, the fracture was assumed to have completely closed at the end of GRIS1. That is, the initial pressure buildup during GRI2 should reflect the test-interval volume of 42 liters, corresponding to that at the end of GRI1, assuming no further borehole closure. The simulated pressure for GRI2 and subsequent GRIS2 is shown in Figure 10. The simulated pressure buildup at beginning of GRI2 results in a steeper slope than the observed slope. This suggests that either the wellbore volume increased or that the apparent wellbore slope is affected by gas flow into the fracture. The second option would be consistent with the fact that the fracture did not close completely and is characterized by a fracture permeability that is higher than that of the undisturbed formation.

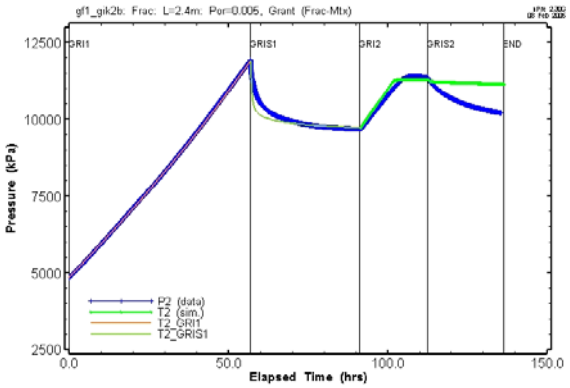

Figure 10: Simulated injection pressures for GRIS1 and GRI2 and GRIS2, assuming a "closed" fracture at the end of GRIS1..

The fracture permeability and corresponding conditions at the end of GRIS1 from the simulation in Figure 9 are used as initial condition for the simulation of the GRI2 sequence. For GRI2, the fracture re-opening was calibrated using a pressure-dependent permeability that varies by a factor of maximal 1,000 over a narrow pressure range between 11.3 and 11.6 MPa. The simulated pressure response shows a nearly linear pressure increase at early time similar to the observed slope (Fig. 11). However, the simulated pressure indicates some deviation from the observed pressure prior to reaching the "re-opening" pressure. The actual re-opening of the fracture represented by the near constant pressure curve, is well reproduced in the simulation (Fig. 11). The calibrated pressure-dependent permeability function for GRI2 does not properly reproduce the GRIS2 response. That is, the apparent fracture permeability decreases over a wider pressure range during the recovery periods GRIS1 and GRIS2 and increases over a narrow pressure interval during GRI2.

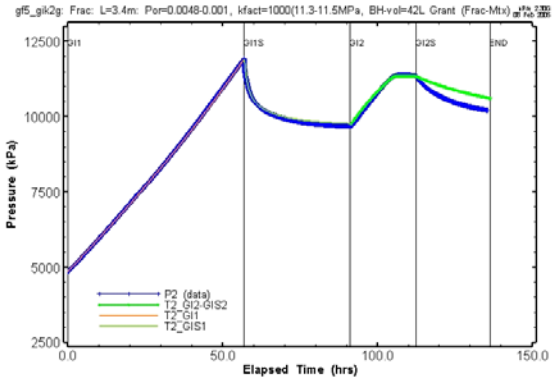

Figure 11: Simulated injection pressures for GRI2 and GRIS2 (calibration of GRI2 response).

Recovery Sequence 2 (GRIS2)

To improve the GRIS2 response, the conditions at the end of GRI2 in Figure 11 are used as initial conditions and the pressure-dependent permeability function is adjusted to improve the fit for GRIS2. The results of this simulation together with those for GRI1 and GRI2 are shown in Figure 12. The inferred permeability changes indicate a non-linear behavior between injection and recovery sequence.

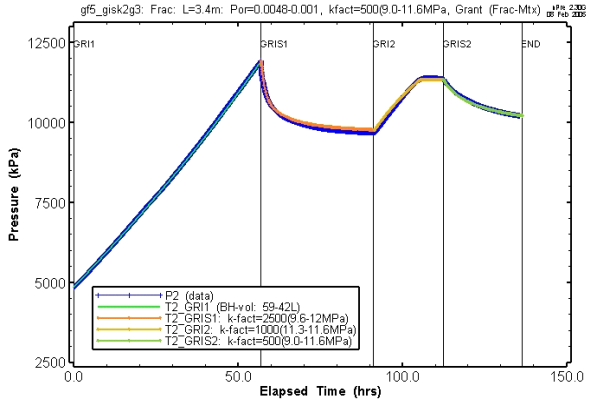

Figure 12: Simulated injection pressures based on calibration of different test sequences.

During GRI2 the permeability increases over a relatively narrow pressure range, whereas during GRIS1 and GRIS2 the permeability changes over a wider pressure range. There is some uncertainty in the inferred pressure ranges and in the multiplication factor for the permeability change due to possible non-uniqueness given the various parameters

associated with the implemented pressure-dependent permeability function. However, the overall behavior is well reproduced.

The simulations indicate that the fracture did not completely close at the end of the recovery period maintaining significantly higher permeabilities compared to that of undisturbed rock. The pulse withdrawal test (PW2) which was conducted at the same pressure level as PW1, following depressurization of the test interval produced essentially the same hydraulic properties as those obtained from the PW1 analysis (Senger et al. 2004). Moreover, the diagnostic plot showed the same characteristics as that shown in Figure 3 for PW1, suggesting that the fracture was completely closed after the depressurization of the test interval following the GTPT.

CONCLUSIONS

The implementation of the mechanical fracture model in the two-phase flow model required assumptions and simplifications. Specific results from the mechanical fracture model, such as fracture aperture and fracture extent, could be incorporated in the numerical model. The aperture varies as a function of distance from the wellbore, which was represented by equivalent fracture porosity for the corresponding radial elements representing the fracture extent. Both the mechanical fracture model and the numerical model assumed a horizontal fracture with radially-symmetric geometry.

The fracture event during the GTPT was implemented in the TOUGH2 model by using the hydraulic conditions at the end of GRI1 as initial conditions in a restart simulation with an instantaneous change in porosity of the elements representing the created fracture. The effect of induced fracturing was approximated by an instantaneous increase in permeability and assuming a Grant relative permeability model for the fracture element. This enabled rapid gas flow from the wellbore into the fracture, displacing the pore water. In addition, the pore water was sucked into the adjacent matrix by the imposed capillary pressure gradient. The fracture extent estimated from the mechanical model had to be extended in the numerical model, mainly to provide initial storage capacity for the gas from the wellbore. However, the total gas volume in the simulation was about 5 liters, which is within the uncertainty range of the fracture volumes estimated from the mechanical model. Thus, the approximation of the fracture mechanics in the two-phase flow model reasonably consistent and reproduces well the observed pressure response. In addition to the fracture behaviour that could be quantified in this study, the initial objective of the GTPT – determining the gas threshold pressure of the undisturbed formation – is also accomplished. The pressure recoveries following the fracturing can be used to extrapolate the gas threshold pressure of the undisturbed formation to (9.5 MPa), which corresponds to an air-entry pressure of 4.5 MPa, based on a static formation pressure of about 5.0 MPa. Without the fracture event, the recovery period would have to be exceedingly long in order to extrapolate the gas threshold pressure.

ACKNOWLEDGMENT

The study has been performed under funding by ANDRA, France, whose support is greatly appreciated.

REFERENCES

Davis, P.M., 1984, Surface deformation associated with a dipping hydrofracture. Journal of Geophysical Research, v. 88, p. 5826-5834.

Davies, P.B., 1991, Evaluation of the role of threshold pressure in controlling flow of waste-generated gas into bedded salt at the Waste Isolation Pilot Plant (WIPP). – Sandia Report, SAND 90-3246.

Finsterle, S., 1999, iTOUGH2 User's Guide, Report LBNL-40040, Lawrence Berkeley National Laboratory, Berkeley, California..

Finsterle, S. and Pruess, K., 1996, Design and analysis of a well test for determining two-phase hydraulic properties. Report LBNL-39620, Lawrence Berkeley National Laboratory, Berkeley, California.

Intera Engineering Ltd., nSIGHTS Version 2.3 User Manual, ERMS# 530161, Sandia National Laboratories, 2005.

Luckner, L., Van Genuchten, M. Th., Nielsen, D., 1989, A consistent set of parametric models for two-phase flow of immiscible fluids in the subsurface, Water Resources Research, 25(10), 2187-2193.

NAGRA, 2001, Sondierbohrung Benken – Untersuchungsbericht, NAGRA NTB 00-01.

Pruess, K., 1991, *TOUGH2* – A General Purpose Numerical Simulator for Multiphase Fluid and Heat Flow, Lawrence Berkeley Laboratory, Report LBL-29400, Berkeley, California.

Senger, R. K., T. Doe, C. Enachescu, 2005, Gas Threshold Pressure Test Interpretation Report, Borehole EST363, Test GTPT1, Andra, Rapport D.RP.0BAK.04.020.

Senger, R.K., Marschall, P., and Lavanchy, J-M., 1999, Gas threshold pressure tests in deep boreholes for determining two-phase flow properties of the host rock at the proposed L/ILW repository, Switzerland. Proceedings on Scientific Basis for Nuclear Waste Management, Materials Research Society, Davos, 1998.